Activation Parameters for the Recombination Reaction of Intramolecular Radical Pairs Generated from the Radical Diffusion-Inhibited HABI Derivative

Sayaka Hatano and Jiro Abe*

Department of Chemistry, School of Science and Engineering, Aoyama Gakuin University, 5-10-1 Fuchinobe, Sagamihara, Kanagawa 229-8558, Japan

Received: March 4, 2008; Revised Manuscript Received: May 1, 2008

Activation parameters were determined for the recombination of radical pairs arising from newly designed, photochromic, radical diffusion-restricted hexaarylbiimidazole (HABI) derivative. We have developed a new type of radical diffusion-inhibited HABI derivative, which contains two equivalent HABI units and yields a tetraradical with four equivalent 2,4,5-triphenylimidazolyl radical (TPIR) units by photoirradiation. This radical dimerization proceeds by a successive first-order reaction from the tetraradical to the parent molecule via a diradical. The rate constants of each reaction were determined from the decay profile of EPR signal intensities. The entropies of activation ($\Delta S^{\ddagger}$) for the first and the successive dimerization steps were estimated to be -178.5 and -205.5 J K^{-1} mol^{-1}, respectively. Within the experimental temperature range, the radical dimerizations are entropy-controlled ($-T\Delta S^{\ddagger} > \Delta H^{\ddagger}$). The large negative $\Delta S^{\ddagger}$ values imply a highly ordered transition state, indicating that the radical dimerizations occur when the TPIR units interact at a specific orientation. The present study demonstrates the availability of radical diffusion-inihibited HABI for the kinetic study of radical−radical reaction.

Introduction

Radical−radical reactions are of particular importance in spin chemistry and bond formation. It is of great significance to investigate the potential energy surface for radical−radical reactions. In general, reliable kinetics data on radical−radical reactions are sparse because these reactions are difficult to study experimentally due to the high reactivity of the chemical species involved. Although experimental studies of the radical−radical reactions for small molecules have been reported by many groups, only a few large aromatic molecules have been the subject of kinetic studies.[1–6] Among the various radical−radical reactions, photodissociation and the following recombination of radical pairs are quite convenient and handy reactions in the condensed phase. The recombination of the radical pairs formed by photodissociation could provide fundamental information on the solvent cage effect as well as on the dynamic behavior of the encounter pair in bimolecular chemistry. Sato et al. investigated the recombination reaction of 2,3,4,5-tetraphenylpyrrolyl radicals (TPPRs), which are colored species of the photochromic reaction of the dimer of TPPR and are remarkably long-lived (more than 10 h) in benzene solution at room temperature.[1] The nonreactive random encounter radical pair, which subsequently separates, is formed by diffusion, while the reactive random encounter radical pair is formed only when TPPRs approach with their reactive sites exactly facing each other. Thus, the diffusion process and the spatial arrangement of the encounter radical pairs complicate the study of the reaction kinetics of the radical−radical reactions in solution. Moreover, the temporal dependence of the concentrations of radical species must be followed since radical−radical reactions generally obey second-order kinetics. We have attempted to overcome these intrinsic difficulties in studying radical−radical reactions by inhibiting the diffusion process of photoinduced radical species from a photochromic system characterized by a reversible photochemical reaction. In this article, we describe the kinetic investigation of the recombination of a diffusion-restricted radical pair arising from the photochromic hexaarylbiimidazole (HABI) derivative.

HABI derivatives, which are well known as photo/thermo/piezochromic materials, have been used as polymerization initiators in industry and have also been investigated spectroscopically since Maeda and Hayashi prepared them.[7] HABIs are readily cleaved, both thermally and photochemically, into a pair of 2,4,5-triphenylimidazolyl radicals (TPIRs), which thermally recombine to reproduce its dimer. The dimer is abbreviated as TPID and is identical to HABI. Indeed, the photochromic behavior of HABIs can be attributed to the photoinduced homolytic reversible cleavage of the C−N bond between the imidazole rings. The high yield of TPIRs in solid matrixes and their low sensitivity to the presence of oxygen stimulated industrial interest in the use of HABIs as a photoinitiator for a wide variety of imaging materials.[8] Though the photochromic behavior of HABI and its derivatives in solution and solid matrixes extensively studied by spectroscopic methods,[9,10] the detailed reaction mechanism of the recombination kinetics including the transition state (TS) is not understood. On the other hand, we have been focusing on the photochromism of HABIs for developing the field of radical chemistry.[10] We have previously reported the in situ direct observation of a photoinduced radical pair in a crystal of 2-(2-chlorophenyl)-1-[2-(2-chlorophenyl)-4,5-di(phenyl)imidazol-2-yl]-4,5-di(phenyl)imidazole (*o*-Cl-HABI) by X-ray diffraction using cryotrapping and also described the first measurements of intermolecular exchange coupling for the photoinduced radical pair by EPR spectroscopy.[10g,i] Our crystallographic study for a single crystal of *o*-Cl-HABI measured after UV irradiation at 103 K has revealed the molecular geometry of the photoinduced radical pair. The resulting spatial arrangement of the radical pair in a

* To whom corresponding should be addressed. E-mail: jiro_abe@chem.aoyama.ac.jp.

10.1021/jp801909k CCC: $40.75
Published on Web 06/18/2008

SCHEME 1: Photochromic Reactions of HABI, 1,8-TPID-naphthalene, and 1C

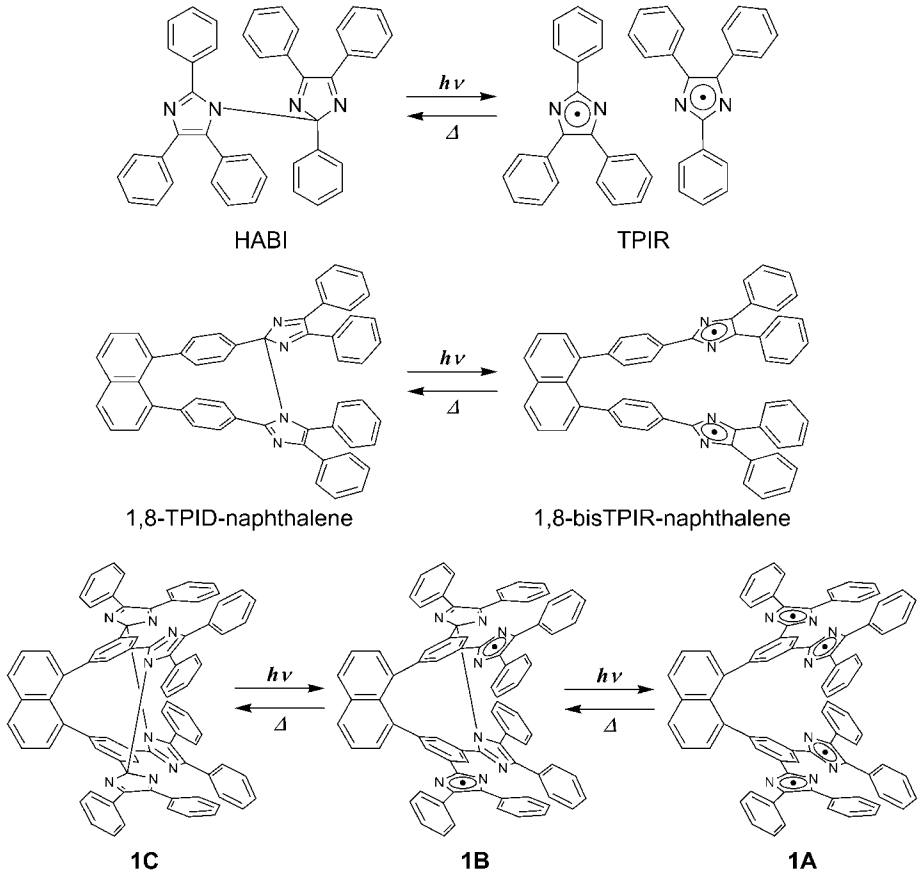

crystal offers a structural suggestion for the TS of the radical dimerization reaction, which will be described in this article.

Recently, we have developed a new class of radical diffusion-inhibited HABI, 1,8-TPID-naphthalene, with the aid of a naphthalene linker as a radical diffusion inhibition unit, as shown in Scheme 1.[10a] 1,8-TPID-naphthalene cleaves photochemically into 1,8-bisTPIR-naphthalene, and the solution changes from colorless to green. Unlike traditional HABI derivatives, the photoinduced radical pair in 1,8-bisTPIR-naphthalene cannot diffuse into the medium to yield free radicals. Therefore, molecular designing applied for the purpose of restricting radical diffusion processes would lead to a new paradigm in the chemistry of radical−radical reactions. A kinetic study of the thermal back-reaction from the diradical, 1,8-bisTPIR-naphthalene, to the dimerized product, 1,8-TPID-naphthalene, showed that the reaction obeys first-order kinetics with a 730 ms half-life in degassed benzene at 298 K. Thus, a drastic acceleration in the recombination reaction of the photoinduced radical pairs was achieved by inhibiting diffusion of the radical pair. This was the first example of a radical diffusion-inhibited system in HABI chemistry.

In this study, we have developed a new type of radical diffusion-inhibited HABI derivative (**1C**), which contains two equivalent HABI units and yields a tetraradical with four equivalent TPIR units by photochemical reaction (Scheme 1). A successive two-step radical dimerization via a diradical (**1B**) should be expected for the tetraradical (**1A**). The first radical−radical reaction of **1A** is considered to result in **1B**, and the successive radical−radical reaction of **1B** yields **1C**. We emphasize that the first and the successive dimerization reactions could be regarded as almost identical radical−radical reactions in that both of them are the radical reaction between two equivalent TPIR units and yield two equivalent HABI units. However, as is distinct from HABI and 1,8-TPID-naphthalene, two TPIR units are located at the meta position of the phenyl ring directly linked to naphthalene ring. Therefore, the bond formation between two TPIR units of **1A** is expected to affect the radical−radical reaction of the other two TPIR units of **1B**. A comparison of the radical dimerization reaction between 1,8-TPID-naphthalene and **1C** is particularly interesting from the standpoint of the control of the radical−radical reaction. We report the synthesis of **1C** and results of the kinetic study for these radical−radical reactions along with the photochromic behavior.

Experimental Section

General. ^{1}H NMR spectra were obtained at 500 MHz with a JMN-ECP500A (JEOL) spectrometer. Chemical shifts are reported in parts per million (ppm) relative to tetramethylsilane, and the coupling constants (J) are reported in hertz (Hz). FAB mass spectra were measured with an MStation MS-700 (JEOL) spectrometer using 3-nitrobenzyl alcohol as a matrix. Elemental analyses were performed with a JM10 micro coder (J-Science), and calibrations were performed using antipyrine. Gel permeation chromatography (GPC) using THF as an eluent was performed with a system composed of a PU-2087 pump (JASCO), a JAIGEL-1H column (2 × 60 cm), and an RI-2031 differential refractometer (JASCO).

Computational Methods. Gaussian 03 (revision D.02) was used for all calculations.[11] Density functional theory (DFT) calculations were performed by the hybrid density functional B3LYP method (the Becke's three parameter hybrid functional with the nonlocal correlation functional of Lee−Yang−Parr) with the 6-31G(d) basis set. The geometries were fully optimized

SCHEME 2: Synthetic Procedure of 1C[a]

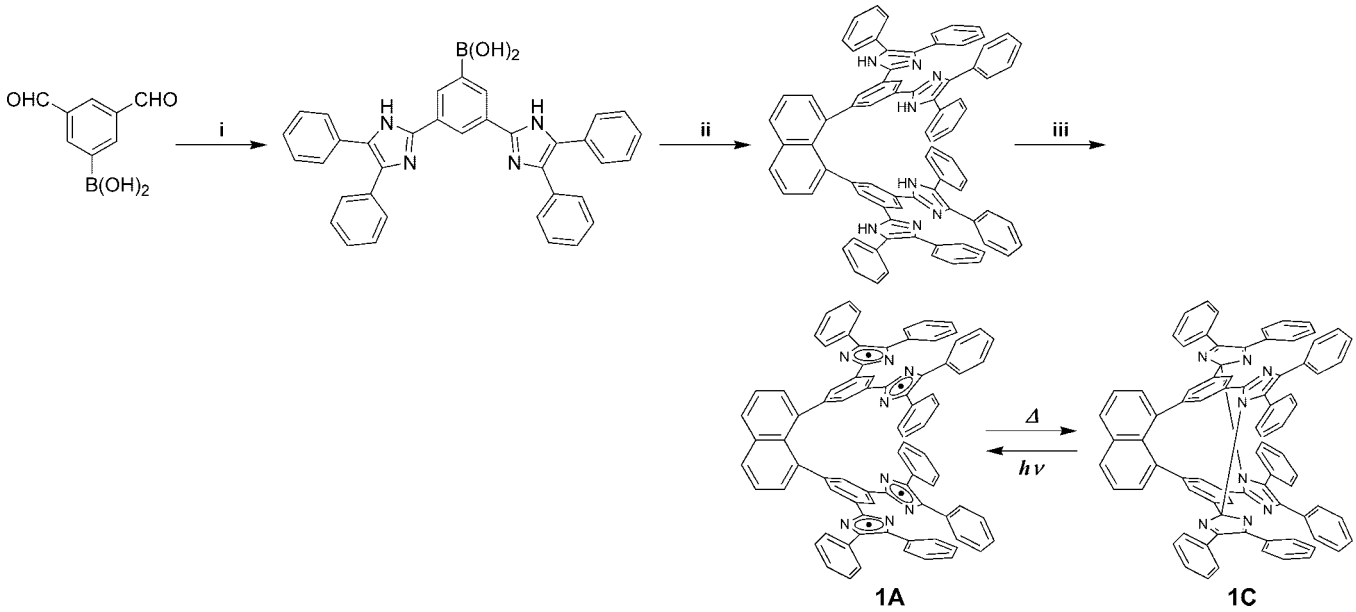

[a] Reagents and conditions: (i) benzil, CH_3COONH_4, CH_3COOH, reflux, 6 h; (ii) diiodonaphthalene, $Pd(PPh_3)_4$, Na_2CO_3(aq), benzene/ethanol, reflux, 1 day; (iii) $K_3[Fe(CN)_6]$, KOH(aq), benzene, r.t., 0.5 h.

with no symmetry or internal coordinate constraints. Analytical frequency calculations at the same level of theory were performed in order to confirm the optimized structures to be a minimum with no imaginary vibrational frequencies as well as to obtain zero-point energy correction.

Measurements. Time-resolved visible-NIR absorption spectra were recorded on an S-2600 diode array spectrophotometer (Soma Optics, Ltd.) over a 400−1000 nm range in a 10 mm × 10 mm quartz cell cooled to the desired temperature in a liquid nitrogen cryostat USP-203-A (Unisoku, Inc.). UV irradiation was carried out using a Keyence UV-400 series UV-LED (UV-50H type), equipped with a UV-L6 lens unit (365 nm, irradiation power 5.4 mW/cm^2). In the measurement of the time-resolved visible-NIR absorption spectra, the sample solutions were bubbled with Ar to remove dissolved oxygen. The solution was vigorously stirred during the irradiation to obtain a coloration as homogeneous as possible. EPR spectra were recorded on a JEOL JES-TE200 spectrometer operating at the X-band equipped with a digital temperature controller model 9650 (Scientific Instruments, Inc.). The sample solution in a quartz tube (ϕ 3.2 mm) was degassed by the freeze−pump−thaw method.

Syntheses. Synthesis of **1C** is outlined in Scheme 2. All reagents except benzil were used as commercially supplied. All reaction solvents were distilled under a nitrogen atmosphere prior to use. Benzil was recrystallized from ethanol. Acetic acid, benzene, and toluene were distilled over appropriate drying reagents prior to use.

[3,5-Bis(4,5-diphenyl-1H-imidazol-2-yl)phenyl]boronic Acid. Under nitrogen, (3,5-diformylphenyl)boronic acid (1.39 g, 7.81 mmol), benzil (4.00 g, 19.0 mmol), and ammonium acetate (59.2 g, 769 mmol) in acetic acid (80 mL) were heated under reflux. After 6 h, the solution was cooled to room temperature and neutralized with aqueous NH_3. The white slurry precipitate formed by neutralization was filtered off, washed with water, and then dried. This residue was purified by silica gel (Wako gel C-300) column chromatography ($CHCl_3$/MeOH = 5:1). [3,5-Bis(4,5-diphenyl-1H-imidazol-2-yl)phenyl]boronic acid was obtained as a white powder (3.69 g, 6.62 mmol, yield 84.7%). ^{1}H NMR (DMSO-d_6, 500 MHz): δ 12.83 (s, 2H), 8.76 (s, 1H), 8.47 (d, 2H), 8.22 (s, 2H), 7.24−7.60 (m, 20H). Anal. Calcd for $C_{36}H_{27}BN_4O_2 \cdot H_2O$: C, 75.01; H, 5.07; N, 9.72. Found: C, 74.64; H, 5.18; N, 9.90.

2,2′,2″,2‴-(Naphthalene-1,8-diyldibenzene-5,1,3-triyl)tetrakis(4,5-diphenyl-1H-imidazole). [3,5-Bis(4,5-diphenyl-1H-imidazol-2-yl)phenyl]boronic acid (2.00 g, 3.59 mmol) and $Pd(PPh_3)_4$ (202 mg, 0.175 mmol) were added to a solution of 1,8-diiodonaphthalene (545 mg, 1.43 mmol) in benzene (95 mL) and ethanol (95 mL) under nitrogen. Sodium carbonate (1.56 g, 14.7 mmol) in water (60 mL) was added to the above solution, and the reaction mixture was refluxed in the dark for 24 h. After cooling to room temperature, the mixture was poured into a mixture of $CHCl_3$ and water. The organic layer was separated, and the aqueous layer was extracted three times with $CHCl_3$. The combined organic layer was washed with water three times and then dried with Na_2SO_4. The solvent was removed under reduced pressure, and the residue was treated by silica gel column chromatography to remove the catalyst. An amount of 1.39 g of the crude product was purified by GPC column chromatography to yield 2,2′,2″,2‴-(naphthalene-1,8-diyldibenzene-5,1,3-triyl)tetrakis(4,5-diphenyl-1H-imidazole) as a yellow powder (773 mg; yield 53.6%). ^{1}H NMR (DMSO-d_6, 500 MHz): δ 12.91 and 13.05 (s, 4H), 7.25−8.87 (m, 52H). FAB MS (*m*/*z*): $[M+H]^+$ calcd for $C_{82}H_{56}N_8$, 1152.46; found, 1153. Anal. Calcd for $C_{82}H_{56}N_8 \cdot 2$(AcOEt): C, 81.30; H, 5.46; N, 8.43. Found: C, 81.17; H, 5.34; N, 8.01.

1C. All manipulations were carried out in the dark. The solution of potassium ferricyanide (4.94 g, 15.0 mmol) and KOH (2.43 g, 43.4 mmol) in water (85 mL) was added to a solution of 2,2′,2″,2‴-(naphthalene-1,8-diyldibenzene-5,1,3-triyl)tetrakis(4,5-diphenyl-1H-imidazole) (860 mg, 0.746 mmol) in benzene (150 mL) under nitrogen. The mixture was vigorously stirred for 0.5 h. After oxidation, the organic layer was separated, washed with water, and concentrated; 808 mg of the crude product of **1C** was obtained, 116 mg of which was purified by preparative thin layer chromatography (PTLC) (SiO_2, 1.0 mm, $CHCl_3$/AcOEt = 20:1) to yield **1C** (44.7 mg; yield 36.2%) as a pale-yellow powder. ^{1}H NMR ($CDCl_3$, 500 MHz): δ 6.50−8.62

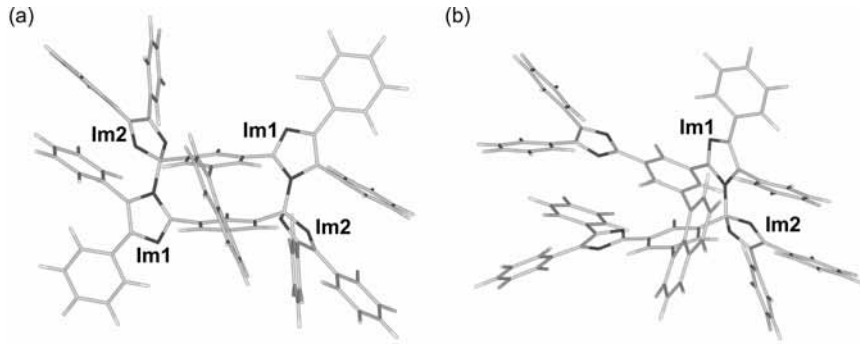

Figure 1. Most stable molecular structures calculated by the B3LYP/6-31G(d) method for (a) **1C** and (b) **1B**.

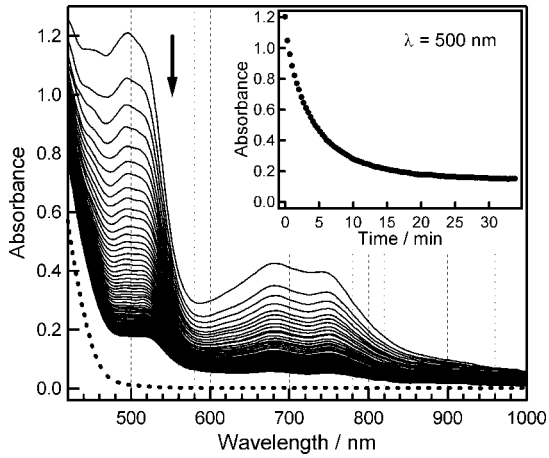

Figure 2. Time-resolved visible−NIR absorption spectrum of the Ar-bubbled solution containing 1.0×10^{-4} mol dm^{-3} **1C** in toluene measured at 253 K immediately after irradiation with 365 nm of UV light in a well-stirred quartz cell (light path length: 10 mm). Spectra were recorded at 20.5 s intervals over a 34 min period. The dashed line indicates the absorption spectrum before UV light irradiation. The inset shows the decay profile of the absorbance at 500 nm.

(m, 52H). Anal. Calcd for $C_{82}H_{52}N_8 \cdot AcOEt$: C, 83.47; H, 4.89; N, 9.06. Found: C, 84.91; H, 4.94; N, 8.42.

Results and Discussion

Theoretical investigations were conducted to confirm the molecular structures of **1C** and **1B**. Spin-unrestricted B3LYP (UB3LYP) theory was used for the singlet state of **1B**. For a wave function derived from the spin-unrestricted DFT calculation, spin contamination is exhibited by a nonzero value of the spin-squared expectation value, $<S^2> = S(S + 1)$, where S is the molecular spin quantum number. We found that the spin contamination for **1B** from states of higher spin multiplicity is low by examining the value of $<S^2>$ (0.3319). The optimized molecular structures are shown in Figure 1. Two imidazolyl rings of **1B** are connected with a C−N bond in a similar manner as that in HABIs,[10d,h,i] tF-BDPI-2YD,[10e] and 1,8-TPID-naphthalene.[10a] One imidazolyl ring (Im1) has a resonant planar structure with the characteristic bond distances for a 6π-electron system, and the other imidazolyl ring (Im2) has two localized C=N double bonds and one sp^3 carbon connecting Im1, consistent with a 4π-electron system. This bonding arrangement is also obtained for **1C**. Thus, it seems reasonable to assume that the first and successive dimerization reactions form the equivalent HABI units.

Upon irradiation with 365 nm light, a pale-yellow solution of **1C** quickly turned to reddish-brown. Figure 2 shows the time-resolved visible−NIR absorption spectrum of **1C** measured at 253 K after irradiation with 365 nm of UV light. The measurement of the time-resolved visible−NIR absorption spectrum was started immediately after ceasing the irradiation when a photostationary state was reached upon UV irradiation. The spectra showed an absorption band centered at 500 nm with a discernible shoulder at longer wavelengths and a broad absorption band with two maximas at about 680 and 750 nm. These absorption bands began to decrease immediately as the irradiation was turned off. Each of the spectra in Figure 2 was recorded at 20.5 s intervals over a 34 min period. These spectra are time-dependent, and the photoinduced transient species disappear via a certain intermediate. For longer times, the shape of the band at around 500 nm broadens, and the intensity of the band at around 460 nm changes. As described in the Introduction, **1C** contains two equivalent HABI units and results in a tetraradical **1A** with four equivalent TPIR units by UV irradiation, and successive two-step radical dimerization via the diradical **1B** is expected for **1A**. Therefore, we considered that the absorption spectrum recorded immediately after light excitation corresponds to that of **1A**, and the intermediate could be assigned to **1B**. From Figure 2, only small differences in the absorption spectra were recognized between **1A** and **1B**. In general, the π-conjugate interaction between two chromophores located at the meta position of a phenyl ring is known to be weak as opposed to the interactions between the para or ortho positions. Therefore, the similarity in the absorption spectra between **1A** and **1B** is understandable by considering the structural features of these radicals. Although **1A** has two units of TPIR, they are located at the meta position. Both of the transitions in the visible wavelength region are attributable to TPIR chromophores. The kinetics for the radical dimerization reaction can be investigated by analyzing the time course of the absorbance of the transient species. As expected from the above considerations, the time dependence of the absorbance did not follow a simple first-order kinetics. We investigated the kinetics for the radical dimerization reaction by EPR spectroscopy, with the expectation of the distinction between **1A** and **1B**. Because the EPR signal intensity is directly propotional to the concentration of paramagnetic species, the time profile of the radical concentration can be followed by the measurement of EPR signal.

Figure 3 shows the decay profile of the normalized EPR signal intensities of **1C** in toluene recorded after the UV light irradiation ceased. The measurements were performed in the temperature range from 281 to 299 K. These decay profiles appear to have fast and slow decay components corresponding to **1A** and **1B**, respectively. The decay of the EPR signals was analyzed assuming that the radical recombination reaction proceeds by the sequential first-order reaction from **1A** to **1C** via **1B**, and the initial concentration of **1B** is negligibly small.

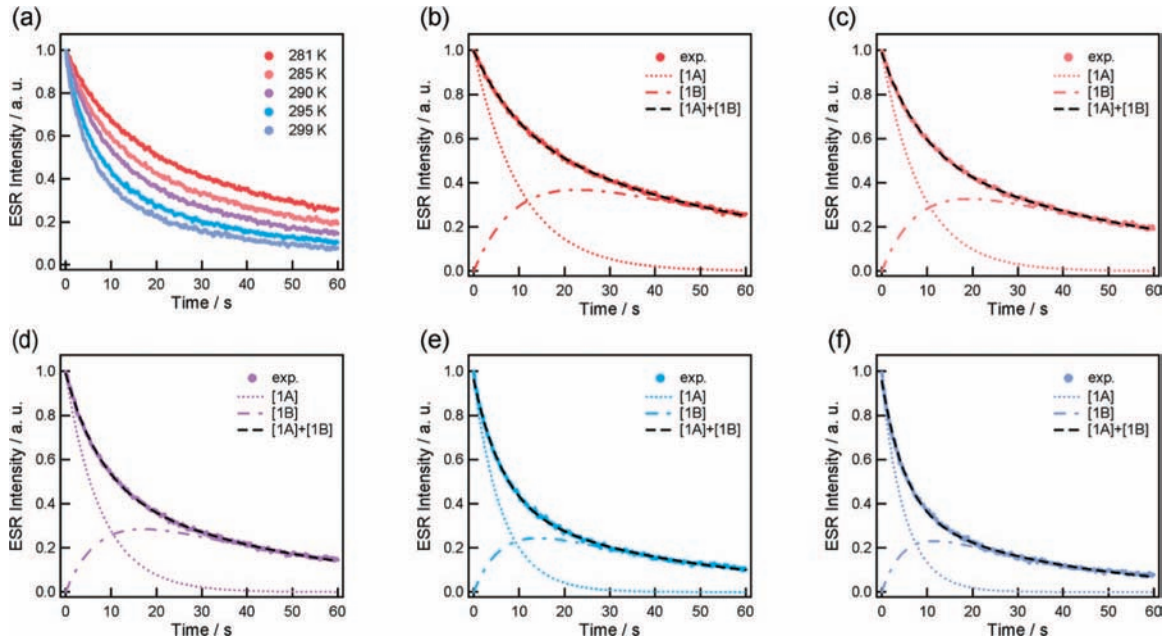

Figure 3. (a) Decay profile of normalized EPR signal intensities of degassed toluene solution of **1C** (1.0×10^{-4} mol dm^{-3}) measured after the UV light irradiation ceased. Time profiles of simulated EPR signal intensities of **1A** and **1B** along with those of the experimental and least-square-fitted intensities measured at (b) 281, (c) 285, (d) 290, (e) 295, and (f) 299 K.

TABLE 1: First-Order Rate Constants for 1A → 1B (k_1) and 1B → 1C (k_2) Estimated from the Decay Profile of the EPR Signal Intensities (where z is a fitting parameter)

T /K	k_1 /s^{-1}	k_2 /s^{-1}	z
281	0.09617	0.015035	1.917
285	0.11499	0.017565	2.154
290	0.12708	0.020580	2.444
295	0.15682	0.023028	2.830
299	0.19621	0.028032	2.991

Therefore, the time profile of the concentration of **1A** and **1B** can be represented as follows

$$[\mathbf{1A}] = [\mathbf{1A}_0]\exp(-k_1 t)$$

$$[\mathbf{1B}] = \frac{k_1}{k_2 - k_1}[\mathbf{1A}_0][\exp(-k_1 t) - \exp(-k_2 t)]$$

Here, k_1 and k_2 stand for the rate constants of **1A** → **1B** and **1B** → **1C**, respectively, and [**1A**$_0$] is the initial concentrarion of **1A**. If both exchange couplings between TPIR units of **1A** and those of **1B** are negligibly small, the EPR signal intensity of **1A** is twice as strong as that of **1B**. However, we analyzed the decay profile of the EPR signal intensities shown in Figure 3a based on the equation of z[**1A**] + [**1B**] instead of 2[**1A**] + [**1B**], where z is a fitting parameter, because the presence of significant exchange coupling between TPIR units cannot be excluded and the line shapes are not necessarily the same for their EPR spectra. The first-order rate constants k_1 and k_2 and the fitting parameter z for the radical dimerization reactions are summarized in Table 1. The z values optimized by the least-squares method ranged from 1.9 at 281 K to 3.0 at 299 K. The time profiles of simulated EPR signal intensities of **1A** and **1B** are shown in Figure 3b−f along with those of the experimental and least-square-fitted intensities.

To further analyze the radical dimerization reactions, the enthalpies and entropies of activation ($\Delta H^{\ddagger}$ and $\Delta S^{\ddagger}$, respectively) were estimated from Eyring plots over temperatures ranging from 281 to 299 K. Both Eyring plots show excellent straight lines, as shown in Figure 4. From standard least-squares

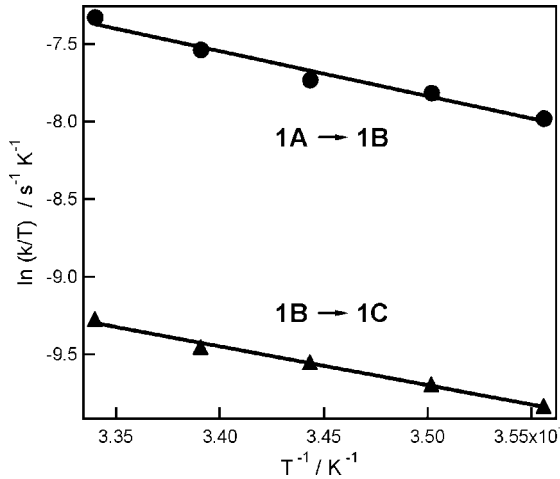

Figure 4. Eyring plots for reactions of **1A** → **1B** and **1B** → **1C** over temperatures ranging from 281 to 299 K.

analysis of the Eyring plots, the $\Delta H^{\ddagger}$ values for the radical dimerization reaction of **1A** → **1B** and of **1B** → **1C** were estimated to be 24.0 and 20.8 kJ mol^{-1}, respectively, and the $\Delta S^{\ddagger}$ values for **1A** → **1B** and **1B** → **1C** were estimated to be −178.5 and −205.5 J K^{-1} mol^{-1}, respectively. It should be noted that both entropy terms, $-T\Delta S^{\ddagger}$, were greater than $\Delta H^{\ddagger}$ at temperatures exceeding 134 K for **1A** → **1B** and 101 K for **1B** → **1C**. Indeed, $-T\Delta S^{\ddagger}$ values of **1A** → **1B** and **1B** → **1C** were approximately 3-fold and 2-fold greater than $\Delta H^{\ddagger}$ at 298 K, respectively. These observations indicate that both radical dimerization reactions are entropy-controlled ($-T\Delta S^{\ddagger} > \Delta H^{\ddagger}$). On the other hand, the radical dimerization reaction of 1,8-bisTPIR-naphthalene is enthalpy-controlled ($-T\Delta S^{\ddagger} < \Delta H^{\ddagger}$) at 298 K since the $\Delta H^{\ddagger}$ and $\Delta S^{\ddagger}$ values are 44.5 kJ mol^{-1} mol^{-1} and −96.2 J K^{-1} mol^{-1}, respectively. Entropy-controlled reactions are not common but have been reported for hydrogen abstraction by a *tert*-butoxyl radical,[12] allylic hydroxylation reaction,[13] additions of carbenes to multiple bonds,[14,15] radical−radical recombination reactions,[16] and enantiomeric Z−E photoisomerization.[17] The large negative $\Delta S^{\ddagger}$ values imply a highly ordered TS, indicating that the radical dimerizations occur when

two TPIR units interact at a specific orientation. The difference in $\Delta S^{\ddagger}$ values between **1A** → **1B** and **1B** → **1C** is of interest because both reactions form equivalent HABI units from equivalent TPIR units. On the basis of the molecular structures of **1B** and **1C**, it is plausible to consider that the bond formation between two TPIR units of **1B** results in a highly ordered TS compared with that of **1A**. These results suggest the possibility of controlling entropy terms of radical−radical reactions with a rational design of the molecular framework.

Conclusion

The results presented in this paper provide new insight into the field of radical−radical reactions. The activation parameters, $\Delta S^{\ddagger}$ and $\Delta H^{\ddagger}$, for the dimerization reaction of TPIR were investigated for the first time. $\Delta S^{\ddagger}$ of the dimerization reaction of TPIR was found to be dependent on the steric orientation around TPIR, and the dimerization reactions showed different $\Delta S^{\ddagger}$ values even for equivalent TPIR units. As described in the Introduction, reliable kinetics data on radical−radical reactions are limited because of the high reactivity of the chemical species involved. The present study demonstrated the availability of radical diffusion-inihibited HABI in the study of radical−radical reactions because side reactions characteristic of radical species can be depressed and the reversible photochromic reaction simplifies various kinetic experiments. In general, it is impossible to control the spatial arrangement of the encounter radical pairs in solution, but this becomes realistic using the molecular framework of radical diffusion-inihibited HABI. In future experiments, intentional control of the spatial arrangement of TPIR units will be attempted to realize another type of bond formation between two TPIR units.

Acknowledgment. This work was supported by a Grant-in-Aid for Science Research in a Priority Area "New Frontiers in Photochromism (No. 471)" from the Ministry of Education, Culture, Sports, Science and Technology, Japan.

Supporting Information Available: Details of DFT calculations for **1B** and **1C**. Absorption spectra of 1,8-TPID-naphthalene and **1C**. Time-resolved visible−NIR absorption spectrum of 1,8-bisTPIR-naphthalene. This material is available free of charge via the Internet at http://pubs.acs.org.

References and Notes

(1) Nakai, T.; Tani, S.; Nishio, S.; Matsuzaki, A.; Sato, H. *J. Phys. Chem. A* **1999**, *103*, 355–361.

(2) Hirata, Y.; Niga, Y.; Makita, S.; Okada, S. *J. Phys. Chem. A* **1997**, *101*, 561–565.

(3) Hirata, Y.; Okada, T.; Mataga, N.; Nomoto, T. *J. Phys. Chem.* **1992**, *96*, 6559–6563.

(4) Hirata, Y.; Ohta, M.; Okada, T.; Mataga, N. *J. Phys. Chem.* **1992**, *96*, 1517–1520.

(5) Graff, M. M.; Wagner, A. F. *J. Chem. Phys.* **1990**, *92*, 2423–2439.

(6) Scott, T. W.; Liu, S. N. *J. Phys. Chem.* **1989**, *93*, 1393–1396.

(7) (a) Hayashi, T.; Maeda, K. *Bull. Chem. Soc. Jpn.* **1960**, *33*, 565–566. (b) Maeda, K.; Hayashi, T. *Bull. Chem. Soc. Jpn.* **1970**, *43*, 429–438.

(8) Monroe, B. M.; Weed, G. C. *Chem. Rev.* **1993**, *93*, 435–448.

(9) (a) White, D. M.; Sonnenberg, J. *J. Am. Chem. Soc.* **1966**, *88*, 3825–3829. (b) Cohen, R. *J. Org. Chem.* **1971**, *36*, 2280–2284. (c) Riem, R. H.; MacLachlan, A.; Coraor, G. R.; Urban, E. J. *J. Org. Chem.* **1971**, *36*, 2272–2275. (d) Cescon, L. A.; Coraor, G. R.; Dessauer, R.; Silversmith, E. F.; Urban, E. J. *J. Org. Chem.* **1971**, *36*, 2262–2267. (e) Tanino, H.; Kondo, T.; Okada, K.; Goto, T. *Bull. Chem. Soc. Jpn.* **1972**, *45*, 1474–1480. (f) Goto, T.; Tanino, H.; Kondo, T. *Chem. Lett.* **1980**, *431*, 434. (g) Lavabre, D.; Levy, G.; Laplante, J. P.; Micheau, J. C. *J. Phys. Chem.* **1988**, *92*, 16–18. (h) Qin, X.-Z.; Liu, A.; Trifunac, A. D.; Krongauz, V. V. *J. Phys. Chem.* **1991**, *95*, 5822–5826. (i) Liu, A.; Trifunac, A. D.; Krongauz, V. V. *J. Phys. Chem.* **1992**, *96*, 207–211. (j) Lin, Y.; Liu, A.; Trifunac, A. D.; Krongauz, V. V. *Chem. Phys. Lett.* **1992**, *198*, 200–206. (k) Morita, H.; Minagawa, S. *J. Photopolym. Sci. Technol.* **1992**, *5*, 551–556. (l) Weidong, Y.; Yongyuan, Y.; Junshen, W.; Cunlin, Z.; Meiwen, Y. *J. Photopolym. Sci. Technol.* **1994**, *7*, 1870–192. (m) Ma, S.; Nebe, W. J. *J. Imaging Sci. Technol.* **1993**, *37*, 498–504. (n) Caspar, J. V.; Khudyakov, I. V.; Turro, N. J.; Weed, G. C. *Macromolecules* **1995**, *28*, 636–641. (o) Oliver, E. W.; Evans, D. H.; Caspar, J. V. *J. Electroanal. Chem.* **1996**, *403*, 153–158. (p) Okada, K.; Imamura, K.; Oda, M.; Kozaki, M.; Morimoto, Y.; Ishino, K.; Tashiro, K. *Chem. Lett.* **1998**, *891*, 892.

(10) (a) Iwahori, F.; Hatano, S.; Abe, J. *J. Phys. Org. Chem.* **2007**, *20*, 857–863. (b) Satoh, Y.; Ishibashi, Y.; Ito, S.; Nagasawa, Y.; Miyasaka, H.; Chosrowjan, H.; Taniguchi, S.; Mataga, N.; Kato, D.; Kikuchi, A.; Abe, J. *Chem. Phys. Lett.* **2007**, *448*, 228–231. (c) Miyamoto, Y.; Kikuchi, A.; Iwahori, F.; Abe, J. *J. Phys. Chem. A* **2005**, *109*, 10183–10188. (d) Nakahara, I.; Kikuchi, A.; Iwahori, F.; Abe, J. *Chem. Phys. Lett.* **2005**, *402*, 107–110. (e) Kikuchi, A.; Iwahori, F.; Abe, J. *J. Am. Chem. Soc.* **2004**, *126*, 6526–6527. (f) Kikuchi, A.; Iyoda, T.; Abe, J. *Chem. Commun.* **2002**, *1484*, 1485. (g) Abe, J.; Sano, T.; Kawano, M.; Ohashi, Y.; Matsushita, M. M.; Iyoda, T. *Angew. Chem., Int. Ed.* **2001**, *40*, 580–582. (h) Kawano, M.; Sano, T.; Abe, J.; Ohashi, Y. *Chem. Lett.* **2000**, 1372–1373. (i) Kawano, M.; Sano, T.; Abe, J.; Ohashi, Y. *J. Am. Chem. Soc.* **1999**, *121*, 8106–8107.

(11) Frisch, M. J. Trucks, G. W.; Schlegel, H. B.; Scuseria, G. E.; Robb, M. A.; Cheeseman, J. R.; Montgomery, J. A., Jr.; Vreven, T.; Kudin, K. N.; Burant, J. C.; Millam, J. M.; Iyengar, S. S.; Tomasi, J.; Barone, V.; Mennucci, B.; Cossi, M.; Scalmani, G.; Rega, N.; Petersson, G. A.; Nakatsuji, H.; Hada, M.; Ehara, M.; Toyota, K.; Fukuda, R.; Hasegawa, J.; Ishida, M.; Nakajima, T.; Honda, Y.; Kitao, O.; Nakai, H.; Klene, M.; Li, X.; Knox, J. E.; Hratchian, H. P.; Cross, J. B.; Bakken, V.; Adamo, C.; Jaramillo, J.; Gomperts, R.; Stratmann, R. E.; Yazyev, O.; Austin, A. J.; Cammi, R.; Pomelli, C.; Ochterski, J. W.; Ayala, P. Y.; Morokuma, K.; Voth, G. A.; Salvador, P.; Dannenberg, J. J.; Zakrzewski, V. G.; Dapprich, S.; Daniels, A. D.; Strain, M. C.; Farkas, O.; Malick, D. K.; Rabuck, A. D.; Raghavachari, K.; Foresman, J. B.; Ortiz, J. V.; Cui, Q.; Baboul, A. G.; Clifford, S.; Cioslowski, J.; Stefanov, B. B.; Liu, G.; Liashenko, A.; Piskorz, P.; Komaromi, I.; Martin, R. L.; Fox, D. J.; Keith, T.; Al-Laham, M. A.; Peng, C. Y.; Nanayakkara, A.; Challacombe, M.; Gill, P. M. W.; Johnson, B.; Chen, W.; Wong, M. W.; Gonzalez, C.; Pople, J. A. *Gaussian 03*, revision D.02; Gaussian, Inc.: Wallingford, CT, 2004.

(12) Finn, M.; Friedline, R.; Suleman, N. K.; Wohl, C. J.; Tanko, J. M. *J. Am. Chem. Soc.* **2004**, *126*, 7578–7584.

(13) Takahashi, A.; Kurahashi, T.; Fujii, H. *Inorg. Chem.* **2007**, *46*, 6227–6229.

(14) Moss, R. A.; Lawrynowicz, W.; Turro, N. J.; Gould, I. R.; Cha, Y. *J. Am. Chem. Soc.* **1986**, *108*, 7028–7032.

(15) Houk, K. N.; Rondan, N. G. *J. Am. Chem. Soc.* **1984**, *106*, 4293–4294.

(16) Sobek, J.; Martschke, R.; Fischer, H. *J. Am. Chem. Soc.* **2001**, *123*, 2849–2857.

(17) Inoue, Y.; Ikeda, H.; Kaneda, M.; Sumimura, T.; Everitt, S. R.; Wada, T. *J. Am. Chem. Soc.* **2000**, *122*, 406–407.

JP801909K